



Article

Co₃Gd₄ Cage as Magnetic Refrigerant and Co₃Dy₃ Cage Showing Slow Relaxation of Magnetisation

 Javeed Ahmad Sheikh ^{1,2,*} , Himanshu Sekhar Jena ^{2,3}  and Sanjit Konar ^{2,*}
¹ Department of Chemistry, Government, College for Women, Constituent College of Cluster University, M. A. Road, Srinagar 190001, Jammu and Kashmir, India

² Department of Chemistry, IISER Bhopal, Bhopal By-Pass Road, Bhopal 462066, Madhya Pradesh, India; himanshu.jena@ugent.be or hsjena@gmail.com

³ Department of Chemistry, Ghent University, Krijgslaan 281-S3 B, 9000 Ghent, Belgium

* Correspondence: javeedsheikh@gcwmaroad.edu.in (J.A.S.); skonar@iiserb.ac.in (S.K.); Tel.: +91-7889872799 (J.A.S.)

Abstract: Two structurally dissimilar 3d-4f cages having the formulae [(Co^{III})₃Gd₄(μ₃-OH)₂(CO₃(O₂C^tBu)₁₁(teaH)₃)]·5H₂O (**1**) and [(Co^{III})₃Dy₃(μ₃-OH)₄(O₂C^tBu)₆(teaH)₃](NO₃)₂·H₂O (**2**) have been isolated under similar reaction conditions and stoichiometry of the reactants. The most important factor for structural diversity seems to be the incorporation of one μ₃-carbonate anion in **1** and not in **2**. Co atoms are in a +3 oxidation state in both complexes, as shown by the Bond Valence Sum (BVS) calculations and bond lengths, and as further supported by magnetic measurements. Co₃Gd₄ displays a significant magnetocaloric effect (−ΔS_m = 25.67 J kg^{−1} K^{−1}), and Co₃Dy₃ shows a single molecule magnet (SMM) behavior.

Keywords: coordination cluster; single molecular magnet; magnetic refrigerant; cages



Citation: Sheikh, J.A.; Jena, H.S.; Konar, S. Co₃Gd₄ Cage as Magnetic Refrigerant and Co₃Dy₃ Cage Showing Slow Relaxation of Magnetisation. *Molecules* **2022**, *27*, 1130. <https://doi.org/10.3390/molecules27031130>

Academic Editor: Luis Cunha-Silva

Received: 20 December 2021

Accepted: 1 February 2022

Published: 8 February 2022

Publisher's Note: MDPI stays neutral with regard to jurisdictional claims in published maps and institutional affiliations.



Copyright: © 2022 by the authors. Licensee MDPI, Basel, Switzerland. This article is an open access article distributed under the terms and conditions of the Creative Commons Attribution (CC BY) license (<https://creativecommons.org/licenses/by/4.0/>).

1. Introduction

The study of nanoscopic paramagnetic metal-ion aggregates has excelled in the last decade or so, not only because of aesthetically pleasing structures but also because of their potential technological applications such as quantum computing [1–3], ultra-high-density data storage [4–9], molecular spintronics [10] and magnetic refrigeration [11–15]. In the field of magnetochemistry, molecular nanomagnets based on Gadolinium show magnetic refrigeration based on the magnetocaloric effect (MCE) [16–19]. Some of the molecular magnetic aggregates that are particularly based on Dysprosium are also useful as single-molecule magnets (SMMs) [20–30].

Polymetallic 3d-4f systems have developed as a fascinating sub-area of research in magnetism [31–45]. Accordingly, a large number of multinuclear 3d-4f cages have been reported in the literature, mainly with carboxylate, tripodal alkoxides and related ligands [31,35–40]. The inclusion of 4f ions (e.g., Dy³⁺, Tb³⁺, etc.) with 3d metals in nanosized systems (3d–4f approach) has been used to incorporate a large number of unpaired f electrons and high intrinsic magnetic anisotropy to obtain SMMs. SMMs based on Dy^{III} exceed those of other Ln^{III}-based SMMs, most likely due to their larger *m_J* state (*m_J* = ±15/2), which could lead to an appreciable magnetic moment. Further, Dy^{III} is a Kramer's ion (it has an odd number of f-electrons), indicating that the ground state will always be bistable irrespective of the crystal field symmetry. Gd³⁺ ions are suitable for the MCE, as they have a high isotropic spin, quenched orbital momentum and weak superexchange interactions. Therefore, 3d-Ln cages comprised of Gd^{III} ions are suitable as magnetic refrigerants [11–15,46–48], and those with Dy^{III} ions (anisotropic) are ideal for SMM behaviour [31–45].

Alkoxo ligands such as N-substituted diethanolamines have been widely used in the synthesis of 3d-4f cages with different numbers of metal centers and magnetic

properties [49–52]. Recently, we have reported a series of complexes based on the N-n-butyl-diethanolamine ligand [53]. With the intention of obtaining new heterometallic cages with an increased magnetic density by decreasing the content of non-metallic elements, we used an alkoxo ligand containing more hydroxyl groups (triethanolamine).

2. Results

2.1. Synthesis and Structural Analysis

In this work, we have employed triethanolamine (teaH₃) with the aim of obtaining new heterometallic cages. The use of the said ligand for such systems is rare [54–57]. We have reacted it with a small dimer, [Co₂(μ-OH₂)(O₂C^tBu)₄](HO₂C^tBu)₄ (hereafter: Co₂), and lanthanide salts, and have successfully isolated two complexes with different structural features under similar reaction conditions and stoichiometry of the reactants. The reaction of Co₂ and teaH₃ with Gd(NO₃)₃·6H₂O in a 1:1:1 molar ratio in CH₃CN gave the compound [(Co^{III})₃Gd₄(μ₃-OH)₂(CO₃)(O₂C^tBu)₁₁(teaH)₃].5H₂O (**1**), whereas a similar reaction with Dy(NO₃)₃·6H₂O led to the compound [(Co^{III})₃Dy₃(μ₃-OH)₄(O₂C^tBu)₆(teaH)₃](NO₃)₂·H₂O (**2**).

X-ray crystallography reveals that complex **1** crystallises in the *P*-1 space group and is a heterometallic heptanuclear cage primarily composed of three cobalt centres and four Gd^{III} ions (Figure 1). All three cobalt centres are in a +3 oxidation state, as shown by the Bond valence sum (BVS) calculations and bond lengths [58]. Two μ₃-hydroxo groups and oxygen atoms of one carbonate anion interconnect the metal centres of this heptanuclear core (Figure 2). Peripheral ligation is provided by three doubly deprotonated triethanolamine ligands (teaH). One can observe that N atoms coordinate to the cobalt ions and that oxygens coordinate to the Gd^{III} ions. The central portion is also enveloped by a hydrophobic covering of eleven pivalate ligands bridging in the 2.11 mode. Therefore, all the cobalt ions end up with an octahedral geometry (with O₅N coordination), and the Gd^{III} ions feature a distorted square antiprismatic geometry. The average Co^{III}–O and Co^{III}–N bond lengths are 1.90 (5) and 1.98 (6) Å, respectively, and the average Gd–O bond length is 2.37 (5) Å.

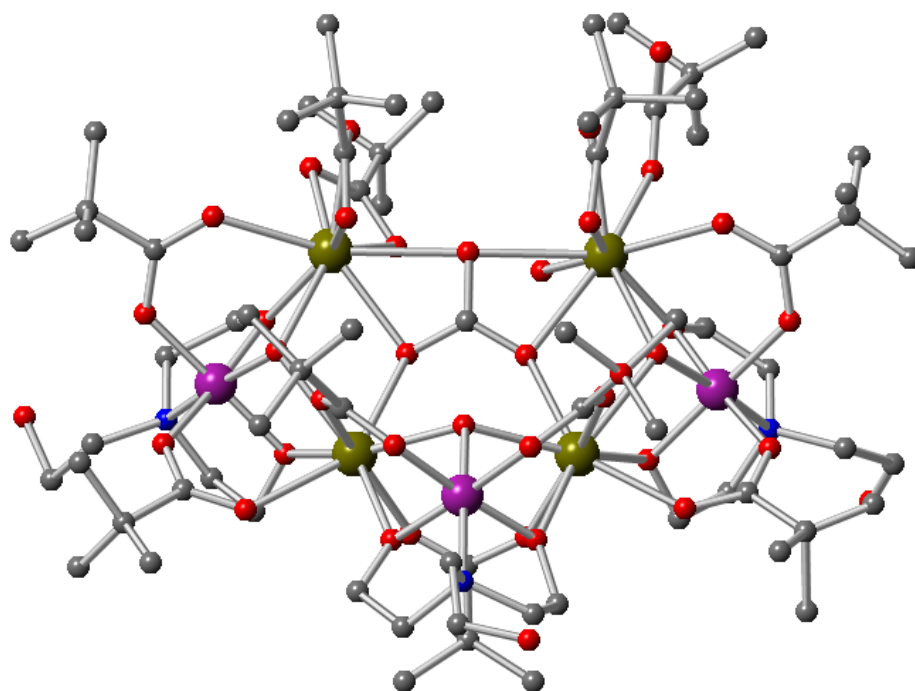


Figure 1. Molecular structure of **1** in the crystal. Colour code: purple, Co^{III}; olive, Gd^{III}; red, oxygen; blue, nitrogen; grey, carbon; Hydrogen atoms are omitted for clarity.

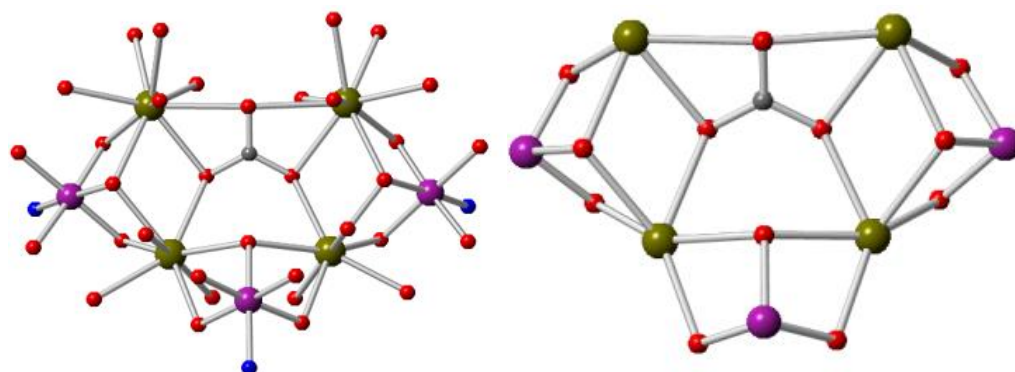


Figure 2. Core structure of **1** (left). Colour code: same as Figure 1. View of the fine core (right).

Complex **2** crystallises in the monoclinic space group $P21/c$ and is another example of a mixed metal system comprising three Co^{III} and three Dy^{III} ions (Figure 3).

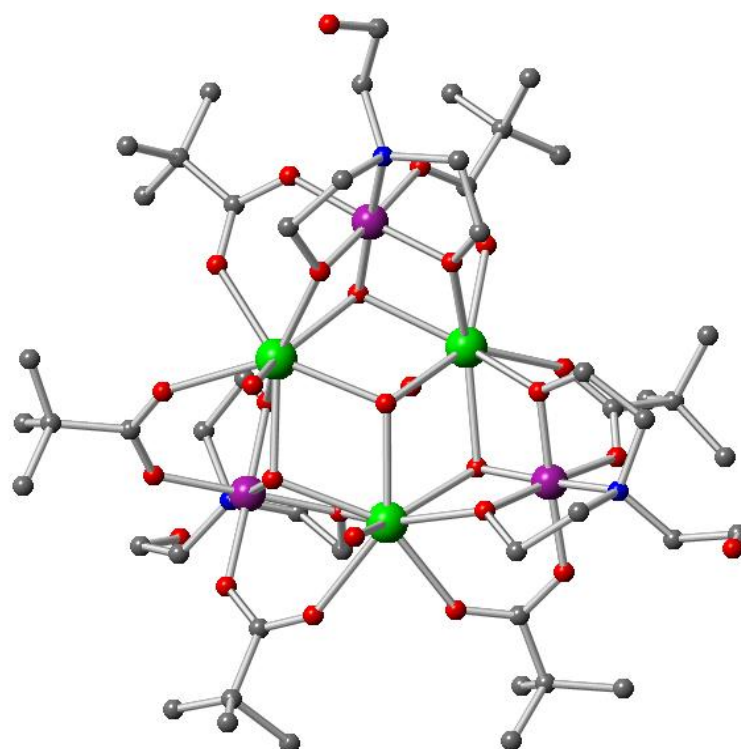


Figure 3. Molecular structure of **2** in the crystal. Colour code: purple, Co^{III} ; green, Dy^{III} ; red, oxygen; blue, nitrogen; grey, carbon; Hydrogen atoms are omitted for clarity.

The metal centres and oxygen atoms in the central hexanuclear unit are interlinked in a hemicubane-like fashion by four μ_3 -hydroxo groups (Figure 4). Three doubly deprotonated triethanolamine ligands (teaH) are also part of this structural aggregation, coordinating via the N atom to the Co^{III} ions and then bridging the Co^{III} centres to the Dy^{III} ions via their two μ_2 -alkoxo groups. Six pivalate groups bridging in the 2.11 mode and three water molecules, one each coordinating to the Dy^{III} ions, also surround the basic unit. With all these coordinating atoms of the ligands, the Co^{III} ions end up being six-coordinated with an octahedral geometry having average Co–O and Co–N bond distances of 1.90 (1) and 1.97 (2) Å, respectively. All the Dy^{III} ions are eight-coordinated, having a distorted square antiprismatic geometry and average Dy–O bond length of 2.36 (6) Å. The average Co–O–Dy and Dy–O–Dy bond angles are 102 (3) $^\circ$ and 110 (3) $^\circ$, respectively.

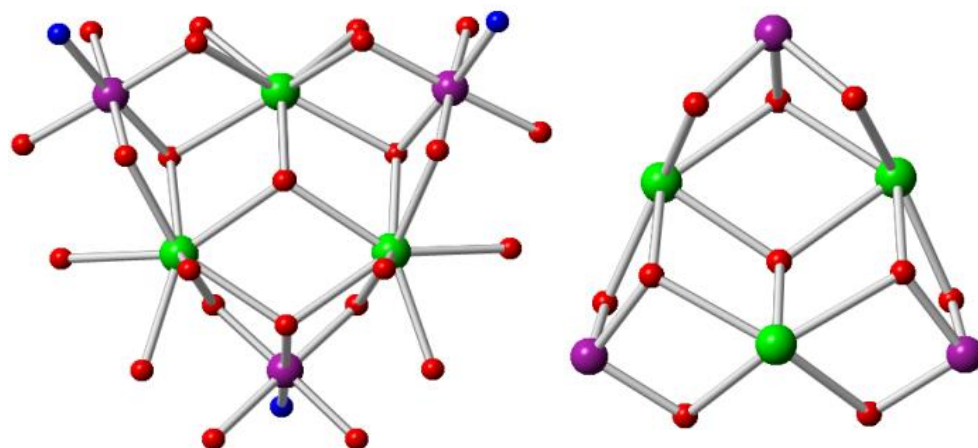


Figure 4. Core structure of **2** (left) and hemicubane-like view of the core (right) Colour code: purple, Co^{III}; green, Dy^{III}; red, oxygen; blue, nitrogen; grey, carbon; Hydrogen atoms are omitted for clarity.

The careful study of the two structures (**1** and **2**) shows some interesting features. Although the number of chelating teaH ligands is the same in both complexes, the number of pivalate groups is reduced to almost half from the former to the latter complex (from 11 in **1** to 6 in **2**). The incorporation of one μ_3 -carbonate anion seems the most important factor for this structural diversity. The number of μ_3 -hydroxo groups is also doubled from two to four from the former to the latter complex, respectively. One μ_3 -hydroxo group is found bridging the three Dy^{III} centres in complex **2** and is not present in complex **1**. Another difference is that each of the Dy^{III} centres in the latter complex is coordinated to one water molecule to complete the coordination sphere.

2.2. Magnetic Studies

Polycrystalline samples of **1** & **2** were used to collect the dc susceptibility data in the temperature range of 1.8–300 K at 0.1 T. The DC magnetic studies (Figure 5) reveal room temperature $\chi_M T$ values of 30.56 and 42.41 cm³ mol⁻¹ K for **1** and **2**, respectively, which are quite close to the estimated values of 29.24 (four uncoupled Gd^{III}, $g = 1.99$) and 42.71 (**2b**, three uncoupled Dy^{III}, $g = 4/3$). Upon lowering the temperature, the $\chi_M T$ products stay nearly constant for complex **1** up to 40 K, where an abrupt decrease is witnessed, reaching a value of 22.89 cm³ mol⁻¹ K at 0.1 T and 1.8 K. This behaviour can be ascribed to the isotropic nature of the Gd^{III} ions. For complex **2**, upon lowering the temperature, the $\chi_M T$ values are nearly constant up to 60 K, followed by an abrupt decrease, reaching a value of 15.75 cm³ mol⁻¹ K at 0.1 T and 1.8 K. This fall could be due to the depopulation of the Stark (m_J) sublevels of the ground J multiplet, with the likelihood of a feeble antiferromagnetic exchange and dipolar interactions also backing the behaviour.

For complex **1**, the field dependence of magnetisation shows a saturation value of 28.8 N μ_B at 7 T (Figure S1). This is compatible with the predicted value of 28 N μ_B . The entropy variations (ΔS_m) for **1** were estimated using the Maxwell equation $\Delta S_m(T)_{\Delta H} = \int [\partial M(T,H)/\partial T]_H dH$ [59]. The $-\Delta S_m$ vs. T plot gradually increases from 9 K to 2 K (Figure 6), reaching a maximum of 25.67 J kg⁻¹ K⁻¹ at 3 K and 7 T. These results compare well with the other Co–Gd cages in the literature [60–63].

The M/N μ_B vs. H plot for **2** (Figure S2) shows an abrupt increase with the increasing field reaching a value of 17.28 N μ_B but not saturating, even at 7 T. This is usually due to the presence of anisotropy and significant crystal field effects from the Dy^{III} ions [54–57]. The non-superposition of the M/N μ_B versus H/T plot of complex **2** (Figure S3) confirms the presence of significant anisotropy in the molecule.

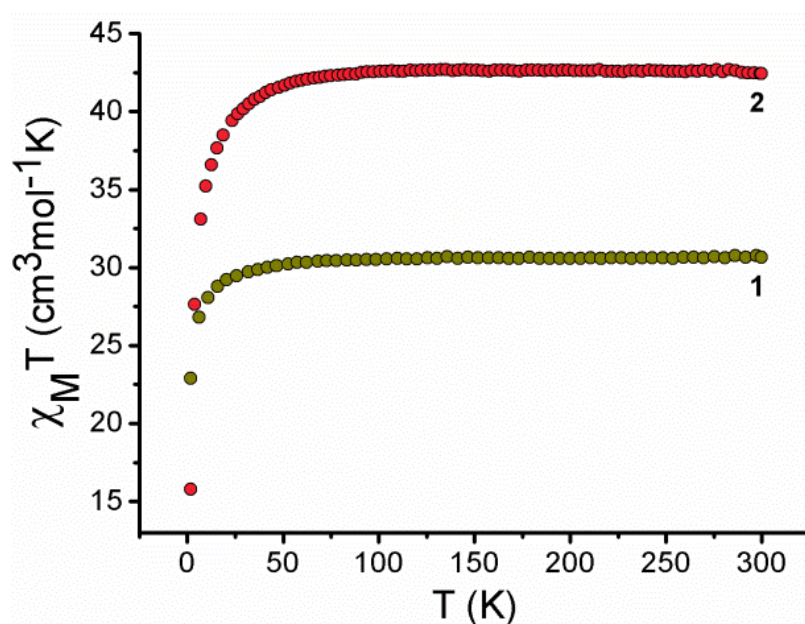


Figure 5. Temperature dependence of $\chi_M T$ measured at 0.1 T for complexes 1 and 2.

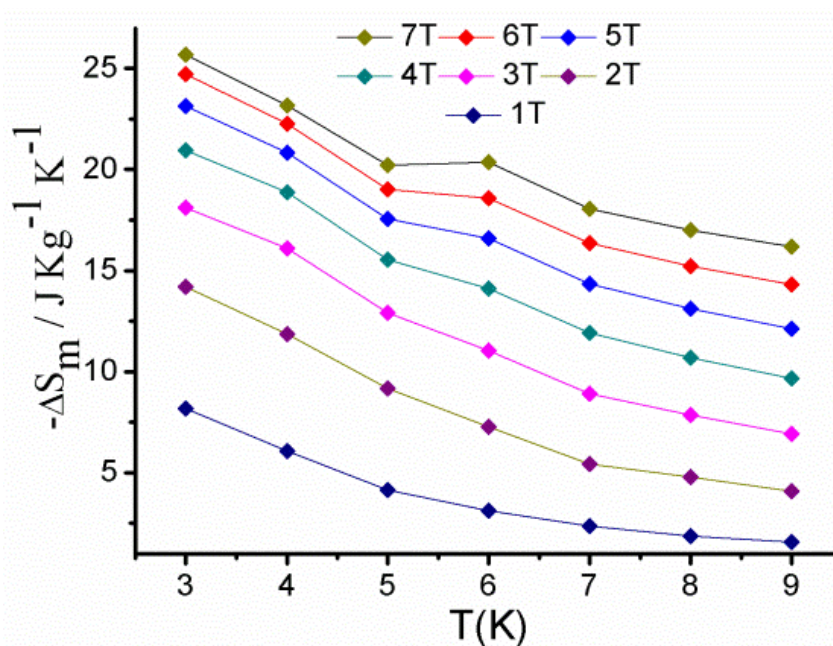


Figure 6. Temperature dependencies (3 to 10 K) of the magnetic entropy change ($-\Delta S_m$) for complex 1, as obtained from magnetisation data.

Alternating current susceptibility data for **2** was collected at a zero dc field up to 1.8 K at the 3.5 Oe ac field in the frequency range of 1–800 Hz. Both the in-phase and out-of-phase susceptibilities show temperature-dependent ac signals below 10 K (Figures S4 and S5), indicating the slow relaxation of magnetisation. Due to quantum tunnelling of the magnetisation (QTM), no full maxima were observed [64,65]. The data was remeasured in the presence of an optimum static dc field of 2000 Oe to minimise the quantum tunnelling. Peak maxima were observed under this field below 5 K in the out-of-phase (χ'') vs. T plot (Figure 7 (left)), confirming the field-induced SMM behaviour [54–57]. The frequency-dependent in-phase (χ') and out-of-phase (χ'') susceptibility plots also confirmed this behaviour (Figure S7 and Figure 7 (right)). The magnetic properties of this compound

strongly resemble one of our previously reported compounds because of the similar core structure [53].

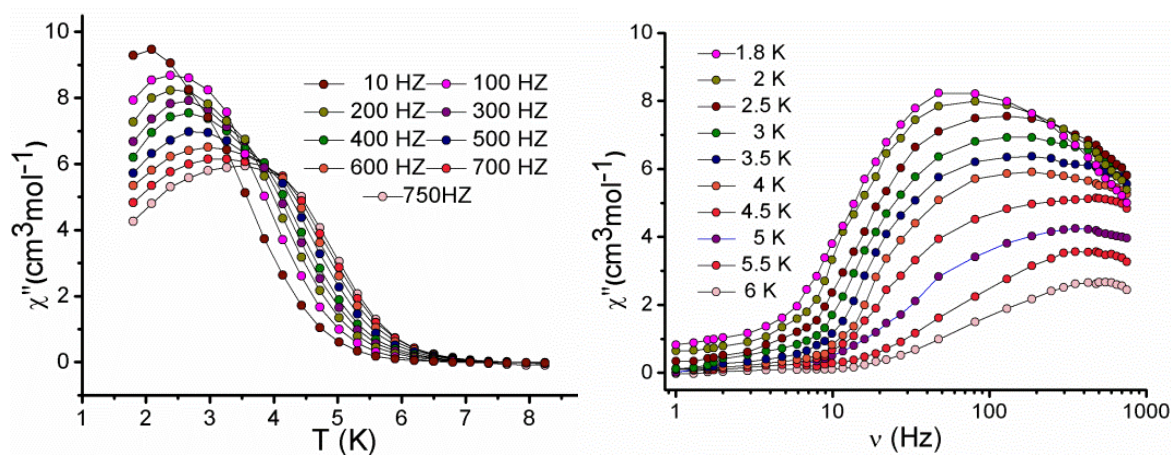


Figure 7. Temperature dependence (left) and frequency dependence (right) of the out-of-phase χ'' ac susceptibility for complex 2 under a 2000 Oe dc field.

The best-fitting results for the Arrhenius equation (Equation (1)) [66,67] gave an energy barrier $U_{\text{eff}} \approx 17.5$ K and a relaxation time $\tau_0 \approx 2.3 \times 10^{-6}$ s from the frequency dependencies of the ac susceptibility (Figure 8).

$$\ln(1/\tau) = \ln(1/\tau_0) - U_{\text{eff}}/kt \quad (1)$$

where k is the Boltzmann constant, and $1/\tau_0$ is the pre-exponential factor.

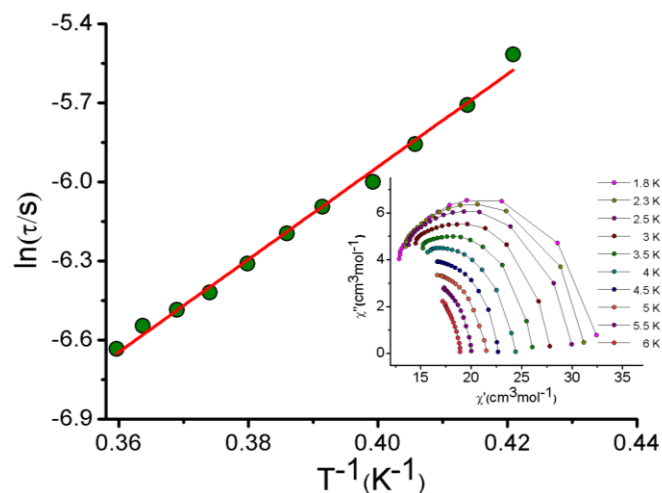


Figure 8. $\ln(1/\tau)$ vs. $1/T$ plot for complex 2. The red line is the best fit for the Arrhenius relationship.

The Cole–Cole plot (χ'' vs. χ') is shown in the inset of Figure 8 as evidence of the relaxation process occurring in complex 2.

3. Materials and Methods

Both complexes were synthesised from the starting material $[\text{Co}_2(\mu\text{-OH}_2)(\text{O}_2\text{C}^t\text{Bu})_4] \cdot (\text{HO}_2\text{C}^t\text{Bu})_4$, Co_2 . All the reagents were used as received from Sigma Aldrich without any further purification. The magnetic behaviour of the compounds was studied on a Quantum Design SQUID-VSM magnetometer. Diamagnetic corrections were made with Pascal's constants for all of the constituent atoms [68]. Magnetic susceptibility measurements were performed in 1.8–300 K with an applied field of 0.1 T. Infrared spectra were collected for

the solid samples using KBr pellets on a Perkin Elmer Fourier-transform infrared (FTIR) spectrometer in the range of 400–4000 cm^{-1} . An Elementar vario Microcube elemental analyser was used to get the elemental analysis data.

Single-crystal X-ray structural studies of **1** & **2** were carried out on a CCD Bruker SMART APEX 2 CCD diffractometer under the cold flow of an Oxford device. Data were collected using graphite–monochromated Mo $K\alpha$ radiation ($\lambda = 0.71073 \text{ \AA}$). Structure solution, refinement and data reduction were carried out by (SHELXTL-97), SAINT and SADABS programs [69–71]. Large solvent accessible voids are present in the structures, which are probably filled with disordered solvent molecules. Therefore, SQUEEZE/PLATON was used to remove or fix these disorders [72]. The CIF format of the data is available in CCDC numbers 1,050,639 and 1,050,640 and is also summarized in Table S2.

4. Conclusions

Two structurally dissimilar heterometallic aggregates were successfully synthesised from a preformed precursor and triethanolamine. The Gd analogue displays a significant magnetocaloric effect, and the Dy-containing compound shows the slow relaxation of the magnetisation. The results are a good addition to the 3d-4f heterometallic aggregates in general and those obtained from polyalcohol-based ligands in particular. This work should be useful to the sensible strategy and production of a library of heterometallic magnetic materials employing different polytopic ligands.

Supplementary Materials: The following supporting information can be downloaded online, Figure S1: Field dependencies of isothermal normalised magnetisations for complex **1** collected for temperatures ranging from 2–10 K. Figure S2: Field dependencies of isothermal normalised magnetisations for complex **2** collected for temperatures ranging from 2–10 K. Figure S3: $M/N\mu_B$ vs. H/T plots for complex **2** at 2–10 K. Figure S4: Temperature dependence of the in-phase (χ') ac susceptibility for complex **2** under a zero dc field. Figure S5: Temperature dependence of the out-of-phase (χ'') ac susceptibility for complex **2** under a zero dc field. Figure S6: Temperature dependence of the in-phase (χ') ac susceptibility for complex **2** under a 2000 Oe dc field. Figure S7: Frequency dependence of the in-phase (χ') ac susceptibility for complex **2** under a 2000 Oe dc field. Table S1: BVS calculations for complexes **1** and **2**. Table S2: Crystal data and structure refinement for complexes **1** and **2**.

Author Contributions: Conceptualization, S.K.; methodology, J.A.S.; software, J.A.S.; validation, J.A.S., S.K. and H.S.J.; investigation, J.A.S.; writing—original draft preparation, J.A.S.; writing—review and editing, H.S.J.; supervision, S.K. All authors have read and agreed to the published version of the manuscript.

Funding: This research received no external funding.

Institutional Review Board Statement: Not applicable.

Informed Consent Statement: Not applicable.

Data Availability Statement: This study did not report any data.

Acknowledgments: J.A.S. acknowledges Government College for Women, M. A. Road, Srinagar for infrastructural support. S.K. thanks D.S.T., Government of India and IISER Bhopal for the generous financial and infrastructural support. H.S.J. thanks Ghent University for support.

Conflicts of Interest: The authors declare no conflict of interest.

References

1. Leuenberger, M.N.; Loss, D. Quantum computing in molecular magnets. *Nature* **2001**, *410*, 789–793. [[CrossRef](#)] [[PubMed](#)]
2. Stamp, P.C.E.; Gaita-Arino, A. Spin-based quantum computers made by chemistry: Hows and whys. *J. Mater. Chem.* **2009**, *19*, 1718–1730. [[CrossRef](#)]
3. Ardavan, A.; Rival, O.; Morton, J.J.L.; Blundell, S.J.; Tyryshkin, A.M.; Timco, G.A.; Winpenny, R.E.P. Will spin-relaxation times in molecular magnets permit quantum information processing? *Phys. Rev. Lett.* **2007**, *98*, 057201. [[CrossRef](#)] [[PubMed](#)]
4. Sessoli, R.; Gatteschi, D.; Caneschi, A.; Novak, M.A. Magnetic bistability in a metal-ion cluster. *Nature* **1993**, *365*, 141–143. [[CrossRef](#)]

5. Gatteschi, D.; Caneschi, A.; Pardi, L.; Sessoli, R. Large clusters of metal ions: The transition from molecular to bulk magnets. *Science* **1994**, *265*, 1054–1058. [[CrossRef](#)]
6. Wernsdorfer, W.; Sessoli, R. Quantum phase interference and parity effects in magnetic molecular clusters. *Science* **1999**, *284*, 133–135. [[CrossRef](#)]
7. Roch, N.; Florens, S.; Bouchiat, V.; Wernsdorfer, W.; Balestro, F. Quantum phase transition in a single-molecule quantum dot. *Nature* **2008**, *453*, 633–637. [[CrossRef](#)]
8. Aromi, G.; Aguila, D.; Gamez, F.; Luis, F.; Roubeauc, O. Design of magnetic coordination complexes for quantum computing. *Chem. Soc. Rev.* **2012**, *41*, 537–546. [[CrossRef](#)]
9. Vincent, R.; Klyatskaya, S.; Ruben, M.; Wernsdorfer, W.; Balestro, F. Electronic read-out of a single nuclear spin using a molecular spin transistor. *Nature* **2012**, *488*, 357–360. [[CrossRef](#)] [[PubMed](#)]
10. Bogani, L.; Wernsdorfer, W. *Nat. Mater.* **2008**, *7*, 179–186.
11. Leng, J.D.; Liu, J.L.; Tong, M.L. Unique nanoscale $\{Cu^{II}_{36}Ln^{III}_{24}\}$ (Ln = Dy and Gd) metallo-rings. *Chem. Commun.* **2012**, *48*, 5286–5288. [[CrossRef](#)] [[PubMed](#)]
12. Evangelisti, M.; Brechin, E.K. Recipes for enhanced molecular cooling. *Dalton Trans.* **2010**, *39*, 4672–4676. [[CrossRef](#)] [[PubMed](#)]
13. Thuesen, A.C.; Pedersen, K.S.; Schau-Magnussen, M.; Evangelisti, M.; Vibenholt, J.; Piligkos, S.; Weihe, H.; Bendix, J. Fluoride-bridged $\{Ln_2Cr_2\}$ polynuclear complexes from semi-labile mer- $[CrF_3(py)_3]$ and $[Ln(hfac)_3(H_2O)_2]$. *Dalton Trans.* **2012**, *41*, 11284–11292. [[CrossRef](#)] [[PubMed](#)]
14. Adhikary, A.; Jena, H.S.; Khatua, S.; Konar, S. Synthesis and Characterization of Two Discrete Ln₁₀ Nanoscopic Ladder-Type Cages: Magnetic Studies Reveal a Significant Cryogenic Magnetocaloric Effect and Slow Magnetic Relaxation. *Chem. Asian J.* **2014**, *9*, 1083–1090. [[CrossRef](#)] [[PubMed](#)]
15. Sheikh, J.A.; Adhikary, A.; Konar, S. Magnetic refrigeration and slow magnetic relaxation in tetranuclear lanthanide cages (Ln = Gd, Dy) with in situ ligand transformation. *New J. Chem.* **2014**, *38*, 3006–3014. [[CrossRef](#)]
16. Warburg, E. Magnetische untersuchungen. *Ann. Phys. Chem.* **1881**, *13*, 141–164. [[CrossRef](#)]
17. Zimm, C.; Jastrab, A.; Sternberg, A.; Pecharsky, V.; Gschneidner, K., Jr.; Osborne, M.; Anderson, I. Description and performance of a near-room temperature magnetic refrigerator. *Adv. Cryog. Eng.* **1998**, *43*, 1759–1766.
18. Pecharsky, V.K.; Gschneidner, K.A., Jr. Magnetocaloric effect and magnetic refrigeration. *J. Magn. Magn. Mater.* **1999**, *200*, 44–56. [[CrossRef](#)]
19. Gschneidner, K.A., Jr.; Pecharsky, V. Thirty years of near room temperature magnetic cooling: Where we are today and future prospects. *Int. J. Refrig.* **2008**, *31*, 945–961. [[CrossRef](#)]
20. Sorace, L.; Benelli, C.; Gatteschi, D. Lanthanides in molecular magnetism: Old tools in a new field. *Chem. Soc. Rev.* **2011**, *40*, 3092–3104. [[CrossRef](#)]
21. Sessoli, R.; Powell, A.K. Strategies towards single molecule magnets based on lanthanide ions. *Coord. Chem. Rev.* **2009**, *253*, 2328–2341. [[CrossRef](#)]
22. Woodruff, D.N.; Winpenny, R.E.P.; Layfield, R.A. Lanthanide single-molecule magnets. *Chem. Rev.* **2013**, *113*, 5110–5148. [[CrossRef](#)] [[PubMed](#)]
23. Feltham, H.L.C.; Brooker, S. Review of purely 4f and mixed-metal nd-4f single-molecule magnets containing only one lanthanide ion. *Coord. Chem. Rev.* **2014**, *276*, 1–33. [[CrossRef](#)]
24. Gatteschi, D.; Sessoli, R.; Cornia, A. Single-molecule magnets based on iron (iii) oxo clusters. Dedicated to the memory of Professor Olivier Kahn. *Chem. Commun.* **2000**, *9*, 725–732. [[CrossRef](#)]
25. Aromí, G.; Brechin, E.K. Synthesis of 3d metallic single-molecule magnets. *Struct. Bond.* **2006**, *122*, 1–67.
26. Glaser, T. Rational design of single-molecule magnets: A supramolecular approach. *Chem. Commun.* **2011**, *47*, 116–130. [[CrossRef](#)] [[PubMed](#)]
27. Rinehart, J.D.; Long, J.R. Exploiting single-ion anisotropy in the design of f-element single-molecule magnets. *Chem. Sci.* **2011**, *2*, 2078–2085. [[CrossRef](#)]
28. Murrie, M. Cobalt (II) single-molecule magnets. *Chem. Soc. Rev.* **2010**, *39*, 1986–1995. [[CrossRef](#)]
29. Vignesh, K.R.; Soncini, A.; Langley, S.K.; Wernsdorfer, W.; Murray, K.S.; Rajaraman, G. Ferrotoroidic ground state in a heterometallic $\{Cr^{III}Dy^{III}_6\}$ complex displaying slow magnetic relaxation. *Nat. Commun.* **2017**, *8*, 1–12. [[CrossRef](#)]
30. Darii, M.; Kravtsov, V.C.; Kramer, K.; Hauser, J.; Decurtins, S.; Liu, S.X.; Affronte, M.; Baca, S.G. Aggregation of a giant bean-like $\{Mn_{26}Dy_6\}$ heterometallic oxo-hydroxo-carboxylate nanosized cluster from a hexanuclear $\{Mn_6\}$ precursor. *Cryst. Growth Des.* **2020**, *20*, 33–38. [[CrossRef](#)]
31. Mondal, K.C.; Sundt, A.; Lan, Y.; Kostakis, G.E.; Waldmann, O.; Ungur, L.; Chibotaru, L.F.; Anson, C.E.; Powell, A.K. Coexistence of Distinct Single-Ion and Exchange-Based Mechanisms for Blocking of Magnetization in a $Co^{II}_2Dy^{III}_2$ Single-Molecule Magnet. *Angew. Chem. Int. Ed.* **2012**, *51*, 7550–7554. [[CrossRef](#)] [[PubMed](#)]
32. Liu, Y.; Ren, Z.C.J.; Zhao, X.Q.; Cheng, P.; Zhao, B. Two-dimensional 3d–4f networks containing planar Co_4Ln_2 clusters with single-molecule-magnet behaviors. *Inorg. Chem.* **2012**, *51*, 7433–7435. [[CrossRef](#)] [[PubMed](#)]
33. Wang, H.S.; Zhang, K.; Song, Y.; Pan, Z.Q. Recent advances in 3d-4f magnetic complexes with several types of non-carboxylate organic ligands. *Inorg. Chim. Acta* **2021**, *521*, 120318. [[CrossRef](#)]
34. Escalera-Moreno, J.; Baldoví, J.; Gaita-Arino, A.; Coronado, E. Spin states, vibrations and spin relaxation in molecular nanomagnets and spin qubits: A critical perspective. *Chem Sci.* **2018**, *13*, 3265–3275. [[CrossRef](#)] [[PubMed](#)]

35. Mishra, A.; Wernsdorfer, W.; Parson, S.; Christou, G.; Brechin, E. The search for 3d–4f single-molecule magnets: Synthesis, structure and magnetic properties of a $[\text{Mn}^{\text{III}}_2\text{Dy}^{\text{III}}_2]$ cluster. *Chem. Commun.* **2005**, *16*, 2086–2088. [[CrossRef](#)] [[PubMed](#)]
36. Mishra, A.; Wernsdorfer, W.; Abboud, K.; Christou, G. Initial observation of magnetization hysteresis and quantum tunneling in mixed manganese–lanthanide single-molecule magnets. *J. Am. Chem. Soc.* **2004**, *126*, 15648–15649. [[CrossRef](#)]
37. Stamatatos, T.C.; Abboud, K.A.; Wernsdorfer, W.; Christou, G. Covalently Linked Dimers of Clusters: Loop-and Dumbbell-Shaped Mn_{24} and Mn_{26} Single-Molecule Magnets. *Angew. Chem. Int. Ed.* **2008**, *120*, 6796–6800. [[CrossRef](#)]
38. Stamatatos, T.C.; Abboud, K.A.; Wernsdorfer, W.; Christou, G. High-Nuclearity, High-Symmetry, High-Spin Molecules: A Mixed-Valence Mn_{10} Cage Possessing Rare T symmetry and an S = 22 Ground State. *Angew. Chem. Int. Ed.* **2006**, *118*, 4240–4243. [[CrossRef](#)]
39. Milios, C.J.; Inglis, R.; Vinslava, A.; Bagai, R.; Wernsdorfer, W.; Parsons, S.; Perlepes, S.P.; Christou, G.; Brechin, E.K. Toward a magnetostructural correlation for a family of Mn_6 SMMs. *J. Am. Chem. Soc.* **2007**, *129*, 12505–12511. [[CrossRef](#)]
40. Chen, W.B.; Chen, Y.C.; Huang, G.Z.; Liu, J.L.; Jia, J.H.; Tong, M.L. Cyclic OFF/Part/ON switching of single-molecule magnet behaviours via multistep single-crystal-to-single-crystal transformation between discrete Fe (ii)–Dy (iii) complexes. *Chem. Commun.* **2018**, *54*, 10886–10889. [[CrossRef](#)]
41. Rigaux, G.; Inglis, R.; Morrison, S.; Prescimone, A.; Cadiou, C.; Evangelisti, M.; Brechin, E.K. Enhancing U eff in oxime-bridged $[\text{Mn}^{\text{III}}_6\text{Ln}^{\text{III}}_2]$ hexagonal prisms. *Dalton Trans.* **2011**, *40*, 4797–4799. [[CrossRef](#)] [[PubMed](#)]
42. Langley, S.K.; Ungur, L.; Chilton, N.F.; Moubaraki, B.; Chibotaru, L.F.; Murray, K.S. Structure, Magnetism and Theory of a Family of Nonanuclear $\text{Cu}^{\text{II}}_5\text{Ln}^{\text{III}}_4$ –Triethanolamine Clusters Displaying Single-Molecule Magnet Behaviour. *Chem. Eur. J.* **2011**, *17*, 9209–9218. [[CrossRef](#)] [[PubMed](#)]
43. Langley, S.K.; Chilton, N.F.; Moubaraki, B.; Hooper, T.; Brechin, E.K.; Evangelisti, M.; Murray, K.S. Molecular coolers: The case for $[\text{Cu}^{\text{II}}_5\text{Gd}^{\text{III}}_4]$. *Chem. Sci.* **2011**, *2*, 1166–1169. [[CrossRef](#)]
44. Li, J.; Wei, R.M.; Pu, T.C.; Cao, F.; Yang, L.; Han, Y.; Zhang, Y.Q.; Zuo, J.L.; Song, Y. Tuning quantum tunnelling of magnetization through 3d–4f magnetic interactions: An alternative approach for manipulating single-molecule magnetism. *Inorg. Chem. Front.* **2017**, *4*, 114–122. [[CrossRef](#)]
45. Schmidt, S.F.M.; Koo, C.; Mereacre, V.; Park, J.; Heermann, D.W.; Kataev, V.; Anson, C.E.; Prodius, D.; Novitchi, G.; Klingeler, R.; et al. A Three-Pronged Attack To Investigate the Electronic Structure of a Family of Ferromagnetic Fe_4Ln_2 Cyclic Coordination Clusters: A Combined Magnetic Susceptibility, High-Field/High-Frequency Electron Paramagnetic Resonance, and ^{57}Fe Mössbauer Study. *Inorg. Chem.* **2017**, *56*, 4796–4806. [[CrossRef](#)] [[PubMed](#)]
46. Zheng, Y.Z.; Evangelisti, M.; Winpenny, R.E.P. Large magnetocaloric effect in a Wells–Dawson type $\{\text{Ni}_6\text{Gd}_6\text{P}_6\}$ cage. *Angew. Chem. Int. Ed.* **2011**, *50*, 3692–3779. [[CrossRef](#)]
47. Zheng, Y.Z.; Evangelisti, M.; Winpenny, R.E.P. Co–Gd phosphonate complexes as magnetic refrigerants. *Chem. Sci.* **2011**, *2*, 99–102. [[CrossRef](#)]
48. Zheng, Y.Z.; Pineda, E.M.; Helliwell, M.; Evangelisti, M.; Winpenny, R.E.P. Mn^{II} – Gd^{III} phosphonate cages with a large magnetocaloric effect. *Chem. Eur. J.* **2012**, *18*, 4161–4165. [[CrossRef](#)]
49. Glaser, T.; Liratzis, I.; Ako, A.M.; Powell, A.K. 2,6-Bis (hydroxymethyl) phenols for the synthesis of high-nuclearity clusters. *Coord. Chem. Rev.* **2009**, *253*, 2296–2305. [[CrossRef](#)]
50. Baniodeh, A.; Hewitt, I.J.; Mereacre, V.; Lan, Y.; Novitchi, G.; Anson, C.E.; Powell, A.K. Heterometallic 20-membered $\{\text{Fe}_{16}\text{Ln}_4\}$ ($\text{Ln} = \text{Sm}, \text{Eu}, \text{Gd}, \text{Tb}, \text{Dy}, \text{Ho}$) metallo-ring aggregates. *Dalton Trans.* **2011**, *40*, 4080–4086. [[CrossRef](#)]
51. Goodwin, J.C.; Sessoli, R.; Gatteschi, D.; Wernsdorfer, W.; Powell, A.K.; Heath, S.L. Towards nanostructured arrays of single molecule magnets: New Fe 19 oxyhydroxide clusters displaying high ground state spins and hysteresis. *J. Chem. Soc. Dalton. Trans.* **2000**, *12*, 1835–1840. [[CrossRef](#)]
52. Brechin, E.K. Using tripodal alcohols to build high-spin molecules and single-molecule magnets. *Chem. Commun.* **2005**, *41*, 5141–5153. [[CrossRef](#)] [[PubMed](#)]
53. Sheikh, J.A.; Goswami, S.; Konar, S. Modulating the magnetic properties by structural modification in a family of Co–Ln ($\text{Ln} = \text{Gd}, \text{Dy}$) molecular aggregates. *Dalton Trans.* **2014**, *43*, 14577–14585. [[CrossRef](#)]
54. Langley, S.K.; Moubaraki, B.; Murray, K.S. A heptadecanuclear $\text{Mn}^{\text{III}}_9\text{Dy}^{\text{III}}_8$ cluster derived from triethanolamine with two edge sharing supertetrahedra as the core and displaying SMM behaviour. *Dalton Trans.* **2010**, *39*, 5066–5069. [[CrossRef](#)] [[PubMed](#)]
55. Chilton, N.F.; Langley, S.K.; Moubaraki, B.; Murray, K.S. Synthesis, structural and magnetic studies of an isostructural family of mixed 3d/4f tetranuclear ‘star’ clusters. *Chem. Commun.* **2010**, *46*, 7787–7789. [[CrossRef](#)] [[PubMed](#)]
56. Langley, S.K.; Chilton, N.F.; Ungur, L.; Moubaraki, B.; Chibotaru, L.F.; Murray, K.S. Heterometallic tetranuclear $[\text{Ln}^{\text{III}}_2\text{Co}^{\text{III}}_2]$ complexes including suppression of quantum tunneling of magnetization in the $[\text{Dy}^{\text{III}}_2\text{Co}^{\text{III}}_2]$ single molecule magnet. *Inorg. Chem.* **2012**, *51*, 11873–11881. [[CrossRef](#)]
57. Langley, S.K.; Chilton, N.F.; Moubaraki, B.; Murray, K.S. Single-molecule magnetism in three related $\{\text{Co}^{\text{III}}_2\text{Dy}^{\text{III}}_2\}$ -acetylacetonate complexes with multiple relaxation mechanisms. *Inorg. Chem.* **2013**, *52*, 7183–7192. [[CrossRef](#)]
58. Liu, W.; Thorp, H.H. Bond valence sum analysis of metal–ligand bond lengths in metalloenzymes and model complexes. 2. Refined distances and other enzymes. *Inorg. Chem.* **1993**, *32*, 4102–4105. [[CrossRef](#)]
59. Phan, M.H.; Yu, S.C. Review of the magnetocaloric effect in manganite materials. *J. Magn. Magn. Mater.* **2007**, *308*, 325–340. [[CrossRef](#)]

60. Zheng, Y.Z.; Evagelisti, M.; Tuna, F.; Winpenny, R.E.P. Co–Ln mixed-metal phosphonate grids and cages as molecular magnetic refrigerants. *J. Am. Chem. Soc.* **2012**, *134*, 1057–1065. [[CrossRef](#)]
61. Pineda, E.M.; Tuna, F.; Pritchard, R.G.; Regan, A.C.; Winpenny, R.E.P.; McInnes, E.J.L. Molecular amino-phosphonate cobalt–lanthanide clusters. *Chem Commun.* **2013**, *49*, 3522–3524. [[CrossRef](#)] [[PubMed](#)]
62. Zhang, Z.M.; Pan, L.Y.; Lin, W.Q.; Leng, J.D.; Guo, F.S.; Chen, Y.C.; Liu, J.L.; Tong, M.L. Wheel-shaped nanoscale 3d–4f {Co^{II}₁₆Ln^{III}₂₄} clusters (Ln = Dy and Gd). *Chem Commun.* **2013**, *49*, 8081–8083. [[CrossRef](#)]
63. Peng, J.B.; Zhang, Q.C.; Kong, X.J.; Zheng, Y.Z.; Ren, Y.P.; Long, L.S.; Huang, R.B.; Zheng, L.S.; Zheng, Z.P. High-nuclearity 3d–4f clusters as enhanced magnetic coolers and molecular magnets. *J. Am. Chem. Soc.* **2012**, *134*, 3314–3317. [[CrossRef](#)] [[PubMed](#)]
64. Layfield, R.A.; McDouall, J.J.W.; Sulway, S.A.; Tuna, F.; Collison, D.; Winpenny, R.E.P. Influence of the N-Bridging Ligand on Magnetic Relaxation in an Organometallic Dysprosium Single-Molecule Magnet. *Chem. Eur. J.* **2010**, *16*, 4442–4446. [[CrossRef](#)]
65. Sulway, S.A.; Layfield, R.A.; Tuna, F.; Wernsdorfer, W.; Winpenny, R.E.P. Single-molecule magnetism in cyclopentadienyl-dysprosium chlorides. *Chem. Commun.* **2012**, *48*, 1508–1510. [[CrossRef](#)] [[PubMed](#)]
66. Xue, S.; Guo, Y.N.; Zhao, L.; Zhang, P.; Tang, J. Unique Y-shaped lanthanide aggregates and single-molecule magnet behaviour for the Dy 4 analogue. *Dalton Trans.* **2014**, *43*, 1564–1570. [[CrossRef](#)] [[PubMed](#)]
67. Chamberlin, R.V.; Orbach, R. Dynamic scaling in the Eu_{0.4}Sr_{0.6}S spin-glass. *Phys. Rev. B* **1984**, *11*, 6514–6520.
68. Kahn, O. *Molecular Magnetism*; Wiley-VCH: New York, NY, USA, 1993.
69. Sheldrick, G. *SHELXL-97, Program for Crystal Structure Refinement*; University of Gottingen: Gottingen, Germany, 1997.
70. *SAINT, Program for Reduction of Area Detector Data*; V6. 63; Bruker-Axs Inc.: Madison, WI, USA, 1999.
71. Sheldrick, G. *SADABS, Program for Absorption Correction of Area Detector Frames*; Bruker-Axs Inc.: Madison, WI, USA, 1996.
72. Speck, A.L. Single crystal structure validation with the program PLATON. *J. Appl. Crystallogr.* **2003**, *36*, 7–13. [[CrossRef](#)]